Hot Electrons

Deutsche Ausgabe: DOI: 10.1002/ange.201603225
Internationale Ausgabe: DOI: 10.1002/anie.201603225

Hot Electrons at Solid–Liquid Interfaces: A Large Chemoelectric Effect during the Catalytic Decomposition of Hydrogen Peroxide

*Ievgen I. Nedrygailov, Changhwan Lee, Song Yi Moon, Hyosun Lee, and Jeong Young Park**

Abstract: *The study of energy and charge transfer during chemical reactions on metals is of great importance for understanding the phenomena involved in heterogeneous catalysis. Despite extensive studies, very little is known about the nature of hot electrons generated at solid–liquid interfaces. Herein, we report remarkable results showing the detection of hot electrons as a chemicurrent generated at the solid–liquid interface during decomposition of hydrogen peroxide (H_2O_2) catalyzed on Schottky nanodiodes. The chemicurrent reflects the activity of the catalytic reaction and the state of the catalyst in real time. We show that the chemicurrent yield can reach values up to 10^{-1} electrons/O_2 molecule, which is notably higher than that for solid–gas reactions on similar nanodiodes.*

Transfer of energetic (hot) charge carriers through a metal–semiconductor (MS) interface plays an important role in many chemical processes.[1] For example, separation of photo-excited electrons and holes at the metal–semiconductor interface can be used to promote various photochemical reactions.[1b,2] Apart from that, the transfer of hot charge carriers may happen through non-adiabatic processes when exothermic reactions take place on the surface of a metal–semiconductor diode.[3] In this case, the movement of charges is a result of direct excitation of electron–hole pairs by the excess chemical energy (ΔE) released during the reaction. Clearly, this process occurs in the absence of any photo-excitation.

In the field of surface chemistry, the detection and utilization of hot electrons generated on metallic surfaces following the deposition of energy have been long-standing issues. The creation of hot electrons by non-adiabatic processes was only confirmed for highly exothermic reactions when the energy transferred to metal electrons was sufficient to allow for electron emission into a vacuum.[1c,3c,4] In the last decade, however, notable progress has also been made toward the study of electronic excitation during low-energy ($\Delta E \approx 1$ eV) reactions catalyzed at a gas–metal interface. Experimental data accumulated to date indicate that the transfer of hot electrons is a common feature of reactions between gaseous reactants and metals where energy is released.[1c,3a–c,5] It is also expected that electronic excitation may be observed for reactions of other types, for example, reactions catalyzed at a liquid–metal interface,[3c,6] which are of tremendous practical importance.[7] However, reliable experimental verification of this hypothesis is lacking thus far.

Herein, we report the direct detection of hot electrons generated at a solid–liquid interface during an exothermic reaction on the surface of metal–semiconductor nanodiodes. To create the hot electrons, catalytic decomposition of hydrogen peroxide (H_2O_2) was used, which is of great importance for a wide range of applications.[8] However, other reactions may also be used in conjunction with this method, provided that the exothermicity of the reaction is large enough to produce hot electrons that are able to overcome the Schottky barrier at the metal–semiconductor boundary.

The principle behind the detection of chemically excited electrons is depicted in Figure 1 a. Hot electrons and holes are generated on the surface of a nanodiode when the chemical reaction takes place. As the electron mean-free path is larger than the thickness of the metal film, hot electrons can reach the metal–semiconductor boundary without significant attenuation. If the energy of the incident electrons exceeds the Schottky barrier, the hot electrons are able to surmount the barrier and generate an electric current, called a chemicurrent. Thus, similar to fuel cells, the nanodiodes are

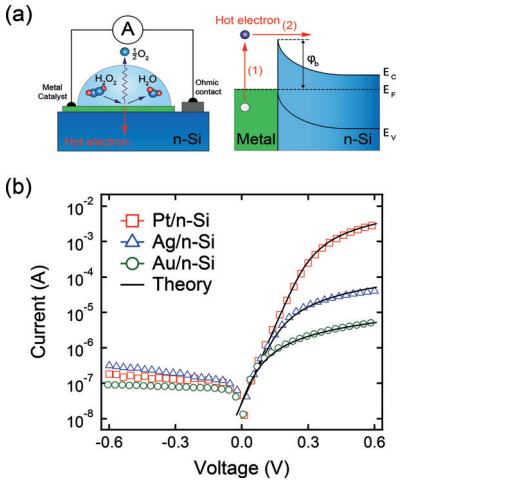

Figure 1. a) Principle of detecting hot electrons during hydrogen peroxide decomposition on a metal/n-Si nanodiode. The basic process involves 1) excitation of a hot electron followed by 2) ballistic transport across the metal–semiconductor contact. b) Typical current–voltage curves measured on the metal/n-Si nanodiodes with Pt, Ag, and Au catalytic films.

[*] I. I. Nedrygailov, C. Lee, S. Y. Moon, H. Lee, Prof. J. Y. Park
Center for Nanomaterials and Chemical Reactions
Institute for Basic Science
Daejeon 305-701 (Korea)
and
Graduate School of EEWS
Korea Advanced Institute of Science and Technology (KAIST)
Daejeon 305-701 (Korea)
E-mail: jeongypark@kaist.ac.kr

Supporting information for this article can be found under: http://dx.doi.org/10.1002/anie.201603225.

converting chemical energy into electrical energy. However, unlike fuel cells where the electric current is composed of positively charged hydrogen ions moving through the electrolyte between the electrodes of a cell, the nanodiodes operate via the transport of highly excited electrons across the electric field at the metal–semiconductor boundary.

Figure 1a shows a schematic diagram of the experiment detecting hot electrons during catalytic decomposition of hydrogen peroxide with metal/n-Si nanodiodes. The roughness and thickness of the metal films are characterized using scanning electron microscopy (SEM) and atomic force microscopy (AFM; Supporting Information, Figure S1). The current–voltage (I–V) curves, shown in Figure 1b, indicate the presence of a potential barrier between the catalytic metals and the n-Si substrate (Supporting Information, Table S1). Note, values obtained for the barrier height are smaller than the energy released during decomposition of H_2O_2 (the standard enthalpy change of reaction $\Delta H = -98.2\ kJ\,mol^{-1} \approx -1.02\ eV$),[9] thus indicating the possibility of using nanodiodes of this type for detecting chemically excited electrons.

When a metal/n-Si nanodiode with a Ag or Pt catalytic film is immersed in an aqueous solution of H_2O_2, catalytic decomposition ($H_2O_2 \xrightarrow{\text{catalyst}} H_2O + {}^1/_2\,O_2$) takes place that is accompanied by intensive oxygen evolution from the metal surface (see the experimental apparatus shown in Figure S2). The last fact is supported by chromatographic analysis (Figure S3). Simultaneous with the catalytic reaction, strong electrical signals are detected from the nanodiodes that are characterized using values of current and electromotive force (EMF), hereinafter referred to as the chemicurrent and chemi-EMF, respectively. Analogous to the thermoelectric and photoelectric effects, let us call this phenomenon the chemoelectric effect. Figure 2a shows typical transients for the chemicurrent measured during decomposition of 3% H_2O_2 (w/w). The largest chemicurrent is detected from the Ag/n-Si nanodiodes. The direction of the chemicurrent corresponds to electron emission from the Ag into the underlying n-Si substrate. The chemicurrent measured from the Pt/n-Si nanodiodes is smaller than that for the Ag/n-Si nanodiodes. However, it remains constant throughout the entire recording time.

Figure 2b shows the time dependence of the chemi-EMF measured across the same nanodiodes during the catalytic decomposition of H_2O_2. In general, the chemi-EMF shows the same trend as the chemicurrent discussed above. Note that the chemicurrent and chemi-EMF are observed only in the case of a catalytic reaction. Nanodiodes immersed in pure water do not lead to any chemoelectric effect (Figure S4). Furthermore, the chemoelectric effect is not observed on the Au/n-Si nanodiodes, which are not active with respect to the decomposition of H_2O_2. The latter fact is clearly seen in Figure 2c, where the rate of oxygen evolution during the H_2O_2 decomposition is shown.

The presence of the stationary chemicurrent in the case of using Pt/n-Si nanodiodes allows for a study of the relationship between detected hot electrons and the surface reaction, which can be done on the basis of the Arrenius equation.[3a,b,10] Figure 3 shows Arrhenius plots obtained from simultaneous measurements of the chemicurrent and the rate of oxygen

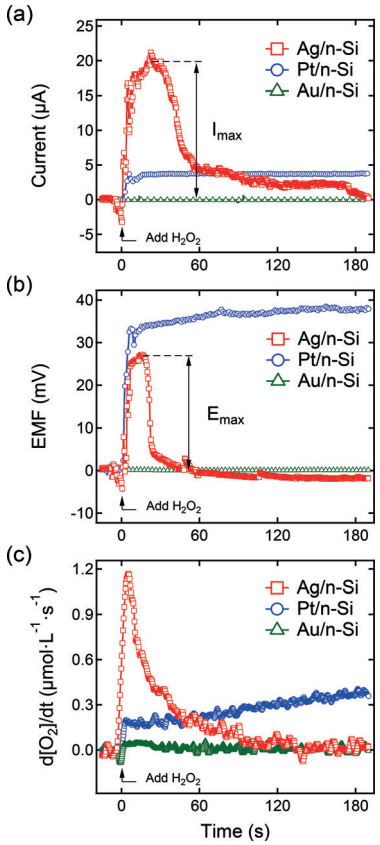

Figure 2. Typical transients of the a) chemicurrent, b) chemi-EMF, and c) rate of oxygen evolution during decomposition of 3% H_2O_2 (w/w) on the metal/n-Si nanodiodes, where "metal" stands for a thin film of Ag, Pt, or Au. The thickness of the metal films is $d = 7 \pm 2$ nm for all nanodiodes. I_{max} and E_{max} denote the peak values of the chemicurrent and EMF.

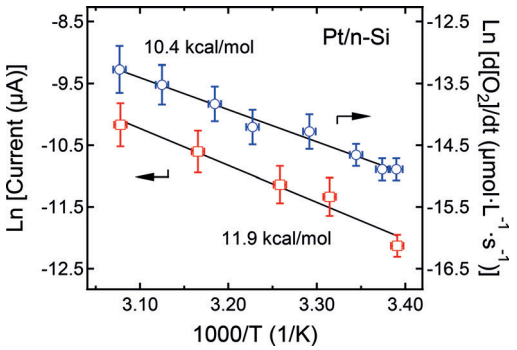

Figure 3. Arrhenius plots obtained from measurements of the chemicurrent and the rate of oxygen evolution during decomposition of 3% H_2O_2 on Pt/n-Si nanodiodes.

evolution. The activation energies determined from the slope of the curves in Figure 3 (11.9 kcal mol^{-1} for chemicurrent and 10.4 kcal mol^{-1} for reaction rate) are in good agreement, which implies that the chemicurrent originates from the catalytic reaction. A slight difference in the values of the activation energy could be attributed to the peculiarities of hot electron transport across the nanodiode.[3a,11]

There are several processes, initiated by a surface reaction, that may lead to electrical signals similar to those shown in Figure 2a,b.[3a,10,12] These include 1) creation of hot electrons from non-adiabatic dissipation of chemical energy;[1c,3a,d,5b,c] 2) chemiluminescence,[1c,4a] which could generate a photocurrent in a nanodiode; and 3) the thermoelectric effect.[12a] Since the chemicurrent composed of hot electrons shows an exponential dependence on the thickness of the catalytic film (i.e. $I = I_o \exp(-d/\lambda_{ch})$, where d is the film thickness and λ_{ch} is the attenuation length), nanodiodes with varied catalytic film thickness can be used to identify the mechanism for current generation (Supporting Information, Section 7).

Figure 4a shows changes in the peak chemicurrent and chemicurrent yield with varying thicknesses of Ag film in the

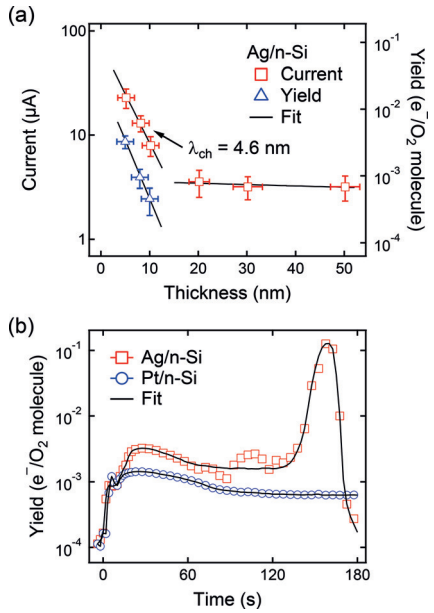

Figure 4. a) Variations of the peak chemicurrent and chemicurrent yield with the thickness of Ag film measured on Ag/n-Si nanodiodes. b) Typical time dependence of the chemicurrent yield for Ag/n-Si and Pt/n-Si nanodiodes. The thickness of the Ag and Pt films is $d = 7 \pm 2$ nm. The black solid lines show a fit based on averaging the data obtained in repeated measurements.

Ag/n-Si nanodiodes. For $d_{Ag} \leq 15$ nm, the chemicurrent decreases with $\lambda_{ch} = 4.6$ nm. However, when further increasing the thickness of the Ag film, the chemicurrent becomes virtually independent of the Ag thickness. In contrast, the thickness dependence of the photocurrent can be characterized by one value of the attenuation length $\lambda_{ph} = 18.1$ nm over the whole range of Ag film thicknesses (Figure S6), which coincides with the data presented in Ref. [5a].

The exponential decrease of the chemicurrent, observed for nanodiodes with Ag thicknesses less than 15 nm, unambiguously indicates that the current is based on hot electrons.[1c,3a,5a,e] In turn, the current measured on the nanodiodes with Ag films thicker than 15 nm is most likely due to the thermoelectric effect. However, further studies are needed for final determination of the nature of this current. Also, based on the attenuation of the photocurrent, we conclude that the current shown in Figure 2a is not based on surface chemiluminescence.

The time-dependent value of the chemicurrent is proportional to the reaction rate, Equation (1) (Supporting Information Section 4)

$$I_{ch} = 2e_0 \alpha \frac{d[O_2]}{dt} A \qquad (1)$$

where e_0 is the elementary charge, α is the yield, and $d[O_2]/dt$ is the rate of O_2 evolution. The physical meaning of α is the number of detected hot electrons per one molecule of product formed during the surface reaction.[1c,3a] Figure 4b shows the yield obtained for Ag/n-Si and Pt/n-Si nanodiodes. In the time interval $t = 0$–90 s, changes in the yield with time are similar for both nanodiodes. At the moment of contact with the solution of H_2O_2 ($t = 0$ s), the yield increases up to values of 10^{-3}–10^{-2} electrons/O_2 molecule. Furthermore, a small flat maximum is observed, which is probably a result of a transitional phase of the chemical reaction when the adsorption and desorption processes become equivalent on the metal surface. However, the behavior of the yield changes significantly for times $t > 90$ s. For the Pt/n-Si nanodiode, the yield reaches a steady-state value of about $\alpha = 6.3 \times 10^{-4}$ electrons/O_2 molecule. In turn, the yield for the Ag/n-Si nanodiode passes through a sharp peak and reaches a record-high value of about $\alpha = 1.2 \times 10^{-1}$ electrons/O_2 molecule. After the peak, the yield drops rapidly to zero. In comparing this behavior with the analysis of SEM images taken from the Ag and Pt surfaces before and after reaction with H_2O_2 (Supporting Information, Section 8), it can clearly be seen that the time dependence of the chemicurrent yield reflects structural changes occurring with the metal films. In particular, the sharp increase in the chemicurrent yield with the successive drop to zero for the case of Ag/n-Si nanodiodes is due to dissolution of the silver film into the H_2O_2 solution, followed by transformation of the Ag film into a system of individual islands.

In summary, we demonstrated the possibility of detecting hot electrons generated by non-adiabatic energy dissipation during catalytic decomposition of H_2O_2 on metal/n-Si nanodiodes. The approach, however, can be used with other exothermic reactions at the liquid–metal interface. Remarkably, the flow of hot electrons (chemicurrent) allows the surface reaction and the state of the catalyst to be monitored in real time. Since both the creation and detection of chemicurrent occur inside the nanodiode, the approach is not limited to specific environmental conditions, as are many other electron-based techniques of surface science that are only capable of operating in a vacuum or at low gas pressures. Thus, this provides a highly sensitive, powerful tool for studying the processes of energy and charge transfer at the interface between liquids and metals. The presented findings may be of interest for a variety of applications including catalysis, electrochemistry, and environmental chemistry.

Acknowledgements

This work was supported by the Institute for Basic Science IBS-R004-G4.

Keywords: hot electrons · hydrogen peroxide · metal-semiconductor interface · Schottky diode · surface reactions

How to cite: *Angew. Chem. Int. Ed.* **2016**, *55*, 10859–10862
Angew. Chem. **2016**, *128*, 11017–11020

[1] a) S. M. Kim, H. Lee, J. Y. Park, *Catal. Lett.* **2015**, *145*, 299–308; b) Z. Zhang, J. T. Yates, Jr., *Chem. Rev.* **2012**, *112*, 5520–5551; c) H. Nienhaus, *Surf. Sci. Rep.* **2002**, *45*, 1–78; d) J. Y. Park, L. R. Baker, G. A. Somorjai, *Chem. Rev.* **2015**, *115*, 2781–2817; e) A. M. Wodtke, D. Matsiev, D. J. Auerbach, *Prog. Surf. Sci.* **2008**, *83*, 167–214; f) D. N. Denzler, C. Frischkorn, C. Hess, M. Wolf, G. Ertl, *Phys. Rev. Lett.* **2003**, *91*, 226102; g) I. I. Nedrygailov, J. Y. Park, *Chem. Phys. Lett.* **2016**, *645*, 5–14.

[2] S. M. Kim, S. J. Lee, S. H. Kim, S. Kwon, K. J. Yee, H. Song, G. A. Somorjai, J. Y. Park, *Nano Lett.* **2013**, *13*, 1352–1358.

[3] a) H. Lee, I. I. Nedrygailov, C. Lee, G. A. Somorjai, J. Y. Park, *Angew. Chem. Int. Ed.* **2015**, *54*, 2340–2344; *Angew. Chem.* **2015**, *127*, 2370–2374; b) A. Hervier, J. R. Renzas, J. Y. Park, G. A. Somorjai, *Nano Lett.* **2009**, *9*, 3930–3933; c) B. Gergen, H. Nienhaus, W. H. Weinberg, E. W. McFarland, *Science* **2001**, *294*, 2521–2523; d) E. G. Karpov, I. Nedrygailov, *Phys. Rev. B* **2010**, *81*, 205443; e) E. Hasselbrink, *Curr. Opin. Solid State Mater. Sci.* **2006**, *10*, 192–204; f) J. W. Gadzuk, *J. Phys. Chem. B* **2002**, *106*, 8265–8270; g) S. N. Maximoff, M. P. Head-Gordon, *Proc. Natl. Acad. Sci. USA* **2009**, *106*, 11460–11465; h) N. Shenvi, H. Cheng, J. C. Tully, *Phys. Rev. A* **2006**, *74*, 062902; i) J. R. Trail, M. C. Graham, D. M. Bird, M. Persson, S. Holloway, *Phys. Rev. Lett.* **2002**, *88*, 166802.

[4] a) T. Greber, *Surf. Sci. Rep.* **1997**, *28*, 1–64; b) B. Kasemo, E. Törnqvist, J. K. Nørskov, B. I. Lundqvist, *Surf. Sci.* **1979**, *89*, 554–565.

[5] a) H. Nienhaus, B. Gergen, W. H. Weinberg, E. W. McFarland, *Surf. Sci.* **2002**, *514*, 172–181; b) J. Y. Park, J. R. Renzas, B. B. Hsu, G. A. Somorjai, *J. Phys. Chem. C* **2007**, *111*, 15331–15336; c) S. K. Dasari, M. A. Hashemian, J. Mohan, E. G. Karpov, *Chem. Phys. Lett.* **2012**, *553*, 47–50; d) B. Mildner, E. Hasselbrink, D. Diesing, *Chem. Phys. Lett.* **2006**, *432*, 133–138; e) B. Schindler, D. Diesing, E. Hasselbrink, *J. Chem. Phys.* **2011**, *134*, 034705; f) Y. Huang, A. M. Wodtke, H. Hou, C. T. Rettner, D. J. Auerbach, *Phys. Rev. Lett.* **2000**, *84*, 2985–2988.

[6] V. V. Styrov, *Tech. Phys. Lett.* **2015**, *41*, 195–199.

[7] F. Zaera, *Chem. Rev.* **2012**, *112*, 2920–2986.

[8] a) Y. Ono, T. Matsumura, N. Kitajima, S. Fukuzumi, *J. Phys. Chem.* **1977**, *81*, 1307–1311; b) N. D. Merkulova, N. A. Zhutaeva, N. A. Shumilova, V. S. Bagotzky, *Electrochim. Acta* **1973**, *18*, 169–174; c) I. Katsounaros, W. B. Schneider, J. C. Meier, U. Benedikt, P. U. Biedermann, A. A. Auer, K. J. J. Mayrhofer, *Phys. Chem. Chem. Phys.* **2012**, *14*, 7384–7391.

[9] M. G. Evans, N. S. Hush, N. Uri, *Q. Rev. Chem. Soc.* **1952**, *6*, 186–196.

[10] J. Y. Park, J. R. Renzas, A. M. Contreras, G. A. Somorjai, *Top. Catal.* **2007**, *46*, 217–222.

[11] H. Lee, I. I. Nedrygailov, Y. K. Lee, C. Lee, H. Choi, J. S. Choi, C.-G. Choi, J. Y. Park, *Nano Lett.* **2016**, *16*, 1650–1656.

[12] a) I. I. Nedrygailov, E. G. Karpov, E. Hasselbrink, D. Diesing, *J. Vac. Sci. Technol. A* **2013**, *31*, 021101; b) J. R. Creighton, M. E. Coltrin, *J. Phys. Chem. C* **2011**, *115*, 1139–1144.

Received: April 1, 2016
Published online: July 4, 2016

